

Intermittency in the Joint Cascade of Energy and Helicity

Qiaoning Chen,¹ Shiyi Chen,^{1,2,3} Gregory L. Eyink,⁴ and Darryl D. Holm^{2,5}

¹Department of Mechanical Engineering, The Johns Hopkins University, Baltimore, Maryland 21218, USA

²Center for Nonlinear Studies and Theoretical Division, Los Alamos National Laboratory, Los Alamos, New Mexico 87545, USA

³CCSE and LTCS, Peking University, China

⁴Department of Mathematical Sciences, The Johns Hopkins University, Baltimore, Maryland 21218 USA

⁵Mathematics Department, Imperial College of Science, Technology and Medicine, London SW7 2AZ, United Kingdom

(Received 31 January 2002; published 30 May 2003)

The statistics of the energy and helicity fluxes in isotropic turbulence are studied using high resolution direct numerical simulation. The scaling exponents of the energy flux agree with those of the transverse velocity structure functions through refined similarity hypothesis, consistent with Kraichnan's prediction. The helicity flux is even more intermittent than the energy flux. Consistent with this observation, the spatial helicity-flux structures are finer than those of energy flux and more tubelike in geometry.

DOI: 10.1103/PhysRevLett.90.214503

PACS numbers: 47.27.Ak, 47.27.Gs

The classical theories of fully developed turbulence [1] were dominated by the concept of the energy cascade to small scales. However, kinetic energy is not the only local conserved integral of the inviscid equations of motion, the three-dimensional (3D) incompressible Euler equations. Since the classical theories were developed, it was discovered [2,3] that there is a second quadratic invariant, the *helicity*:

$$H(t) = \int d\mathbf{x} \mathbf{u}(\mathbf{x}, t) \cdot \boldsymbol{\omega}(\mathbf{x}, t). \quad (1)$$

Here \mathbf{u} is the velocity field and $\boldsymbol{\omega} = \nabla \times \mathbf{u}$ is the vorticity field. Nonzero mean values of the helicity are now known to occur naturally in a wide variety of geophysical flows, such as hurricanes and tornadoes [4]. It was proposed in Refs. [5,6] that, if the large scales of the flow are helical (parity noninvariant), then there should be a *joint cascade* of both energy and helicity to small scales. In that case, the helicity spectrum as well as the energy spectrum should satisfy a $-5/3$ law in the inertial range: $H(k) \sim C_H(\chi/\epsilon^{1/3})k^{-5/3}$. Just as for a passive scalar, the spectrum of helicity was predicted to be linearly proportional to its mean flux χ [7]. In the Gledzer-Ohkitani-Yamada (GOY) shell models, it has been found numerically in Ref. [8] that the scaling exponents of the energy flux are nearly identical to those for 3D Navier-Stokes (NS) precisely for the members of the family which have a "helicity" invariant. The statistics of the "helicity flux" itself have also been studied in the GOY models [9] and in a related class of helical shell models [10]. However, so far the statistics of the helicity flux have yet to be explored in 3D turbulence. It is the purpose of this Letter to study the statistics of energy and helicity fluxes in 3D hydrodynamical turbulence by direct numerical simulations, both with and without a nonzero mean helicity.

We have simulated the NS equation in a 512^3 domain at $Re_\lambda = 210$. The kinetic energy is forced in the first two

shells [11]. To add positive mean helicity into the flow, we rotate the real and imaginary parts of the velocity vector Fourier amplitude also in the first two shells to be always perpendicular to each other with the same handedness [12]. The NS equation was solved using a pseudospectral parallel code with full dealiasing and time stepping by a second-order Adam-Bashforth method. A statistical stationary state was achieved after ten large-eddy turnover times. In Fig. 1 we plot the energy and helicity spectra of this final steady state, in the case with mean helicity input. (See Ref. [13] for appropriate definitions.) Both spectra have about a decade and a half where a $-5/3$ power law holds. In the inset we show for the same simulation the mean spectral fluxes of energy and helicity as a function of wave number, normalized by mean energy dissipation $\epsilon = \nu \langle |\nabla \mathbf{u}|^2 \rangle$ and mean helicity dissipation $\chi = 2\nu \langle \nabla \mathbf{u} : \nabla \boldsymbol{\omega} \rangle$. There is about a decade of inertial range where these fluxes are constant.

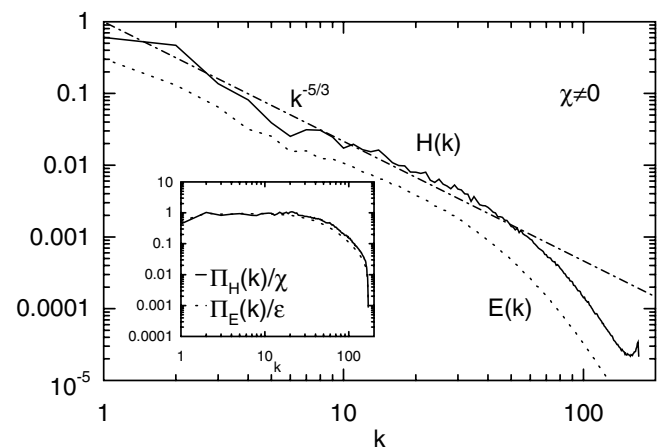


FIG. 1. Energy and helicity spectra. In the inset is shown normalized energy and helicity fluxes.

The importance of a *local energy flux* for studying intermittency in the 3D energy cascade was first emphasized by Kraichnan [14], who used banded Fourier series to define such a quantity. The local flux $\Pi_{E,\Delta}(\mathbf{x})$ measures transfer of energy into small length scales $<\Delta$ at a fixed point \mathbf{x} in physical space. Kraichnan proposed a *refined similarity hypothesis* (RSH) for this quantity, distinct from Kolmogorov's for volume-averaged energy dissipation [15]. The new RSH relates the scaling exponents ζ_p^E of the velocity structure functions, defined as $\langle |\delta_\Delta \mathbf{u}|^p \rangle \sim \Delta^{\zeta_p^E}$, to the scaling exponents τ_p of the energy flux, defined by $\langle |\Pi_{E,\Delta}|^p \rangle \sim \Delta^{\tau_p}$. Here $|\delta_\Delta \mathbf{u}|$ is the magnitude of the vector velocity increment. Precisely, the RSH relation is $\zeta_p^E = \frac{p}{3} + \tau_{p/3}$. Equivalently, this relation may be stated as equality $\zeta_p^E = \zeta_p^E$, with the latter defined by

$$\langle |\Delta \cdot \Pi_{E,\Delta}|^{p/3} \rangle \sim \Delta^{\zeta_p^E} \quad (2)$$

for $L \gg \Delta \gg \eta$, where L is the integral length and η is the dissipation length. To test this relation here, we use instead a smooth filter to differentiate the large-scale and small-scale modes, as in our earlier work [16]. This is the same method used in the large-eddy simulation modeling scheme [17]. A low-pass filtered velocity $\bar{\mathbf{u}} = G_\Delta * \mathbf{u}$ with scales $<\Delta$ removed obeys the equation

$$\partial_t \bar{\mathbf{u}} + (\bar{\mathbf{u}} \cdot \nabla) \bar{\mathbf{u}} = \bar{\mathbf{f}} - \nabla \bar{p} - \nabla \cdot \boldsymbol{\tau} \quad (3)$$

in the limit of high Reynolds number, where viscous terms can be neglected. Here $\bar{\mathbf{f}}$, \bar{p} are the filtered forcing and pressure, respectively, and $\boldsymbol{\tau} = \bar{\mathbf{u}} \otimes \bar{\mathbf{u}} - \bar{\mathbf{u}} \otimes \bar{\mathbf{u}}$ is the *turbulent stress*, or spatial momentum transport induced by the eliminated small-scale turbulence. From this equation, a balance equation is easily derived for the local density $e_\Delta = \frac{1}{2} |\bar{\mathbf{u}}|^2$ of the large-scale energy [16]:

$$\partial_t e_\Delta(\mathbf{x}, t) + \nabla \cdot \mathbf{J}_{E,\Delta}(\mathbf{x}, t) = F_{E,\Delta}(\mathbf{x}, t) - \Pi_{E,\Delta}(\mathbf{x}, t) \quad (4)$$

in which the current $\mathbf{J}_{E,\Delta}$ represents space transport of the large-scale energy, $F_{E,\Delta} = \bar{\mathbf{f}} \cdot \bar{\mathbf{u}}$ is the energy input from the force, and

$$\Pi_{E,\Delta}(\mathbf{x}, t) = -\nabla \bar{\mathbf{u}}(\mathbf{x}, t) : \boldsymbol{\tau}(\mathbf{x}, t) \quad (5)$$

is the *energy flux* out of the large-scale and into the small-scale modes. See also Refs. [18,19].

In the same way, we can derive a balance equation for the density $h_\Delta = \bar{\mathbf{u}} \cdot \bar{\boldsymbol{\omega}}$ of the large-scale helicity:

$$\partial_t h_\Delta(\mathbf{x}, t) + \nabla \cdot \mathbf{J}_{H,\Delta}(\mathbf{x}, t) = F_{H,\Delta}(\mathbf{x}, t) - \Pi_{H,\Delta}(\mathbf{x}, t). \quad (6)$$

Here $\mathbf{J}_{H,\Delta}$ is a space transport of large-scale helicity and $F_{H,\Delta}$ is the input from the forcing, while

$$\Pi_{H,\Delta}(\mathbf{x}, t) = -2 \nabla \bar{\boldsymbol{\omega}}(\mathbf{x}, t) : \boldsymbol{\tau}(\mathbf{x}, t) \quad (7)$$

is the local *helicity flux* to small scales $<\Delta$. A set of scaling exponents ζ_p^H corresponding to the helicity cascade can be defined for $L \gg \Delta \gg \eta$ by

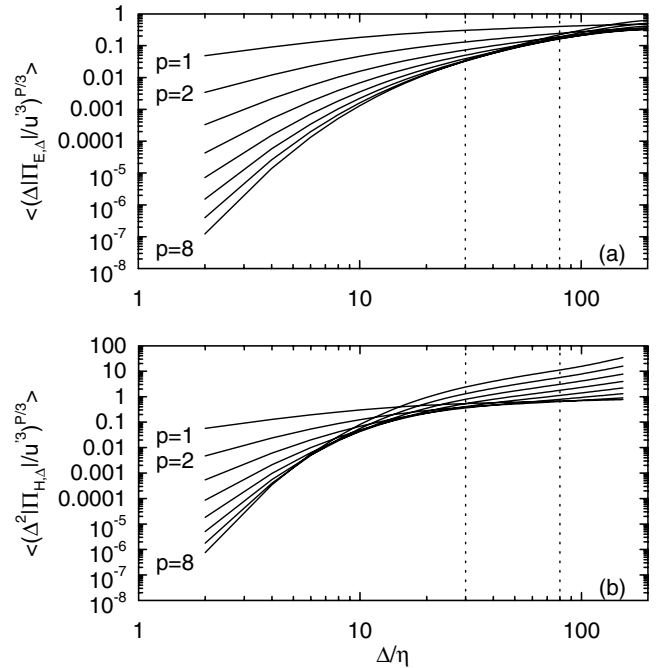


FIG. 2. Structure functions (a) of energy flux and (b) of helicity flux. The dashed lines show constant-flux range $30 \leq \Delta/\eta \leq 80$. u' is rms velocity.

$$\langle |\Delta^2 \Pi_{H,\Delta}|^{p/3} \rangle \sim \Delta^{\zeta_p^H}. \quad (8)$$

In Fig. 2 we plot the structure functions of the energy and helicity fluxes that appear on the left-hand sides of Eqs. (2) and (8) for integer values of p from 1 to 8.

We use the extended self-similarity procedure [20] to extract the scaling exponents ζ_p^E and ζ_p^H from plots against $\langle |\Delta \Pi_{E,\Delta}| / u^3 \rangle$. The results are shown in Fig. 3. Together with these we plot the scaling exponents ζ_p^T of the transverse velocity structure functions. The transverse velocity differences are known to be more intermittent

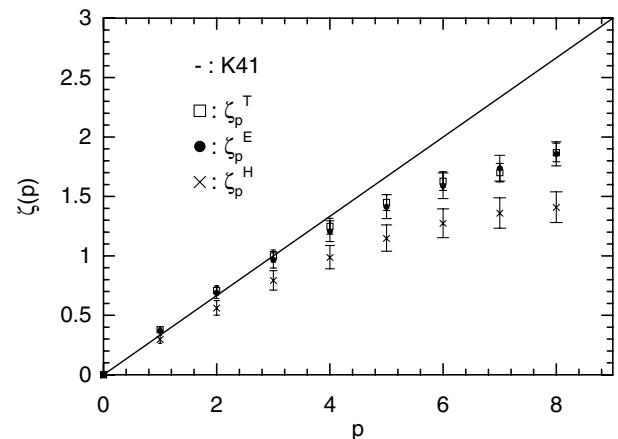


FIG. 3. Scaling exponents of transverse velocity increments, energy flux, and helicity flux.

than the longitudinal ones [21,22] and thus must dominate in the structure function for which Kraichnan's RSH was proposed, which includes *all* velocity components. As may be seen from Fig. 3, the scaling exponents ζ_p^T and ζ_p^E are quite close for each p , in agreement with Kraichnan's RSH [14,16]. However, the scaling exponents for helicity flux are smaller, $\zeta_p^H < \zeta_p^E$, indicating that the helicity flux is intrinsically *more intermittent* than the energy flux, i.e., the departures from K41 scaling are larger. This is consistent with the picture of the helicity acting similarly as a passive scalar, since it is well known that the scaling exponents of the scalar are smaller than those of the advecting velocity itself [23,24]. It is worth emphasizing that the relation between the scaling exponents of energy flux and helicity flux found here is exactly the opposite of that observed in the shell models. In Ref. [9] it was shown numerically that the helicity flux in the GOY shell model is *less* intermittent than the energy flux there, while in [10] it was shown for the helical GOY3 model that energy and helicity fluxes are *equally* intermittent. Thus, despite the fact that the energy flux statistics of the helicity-conserving shell models are very similar to those of 3D Navier-Stokes [8], nevertheless the helicity-flux statistics of these shell models are qualitatively different from those of Navier-Stokes.

Fluctuations of the fluxes $\Pi_{E,\Delta}(\mathbf{x}, t)$ and $\Pi_{H,\Delta}(\mathbf{x}, t)$ in the joint cascade can also be described by the single-point probability density functions (PDF's), which we have calculated at various values of Δ in the inertial range. In Fig. 4 are plotted these PDF's for $\Delta/\eta = 64$. The PDF of the energy flux agrees with the results reported earlier in Ref. [19]. There is an obvious skewness with a long tail to the right, indicating the forward cascade of energy preferentially to smaller scales. To our knowledge, the result on the helicity-flux PDF in Fig. 4 is entirely new. In contrast to the PDF of the energy flux, it is nearly symmetric. This is because the helicity is indefinite in sign

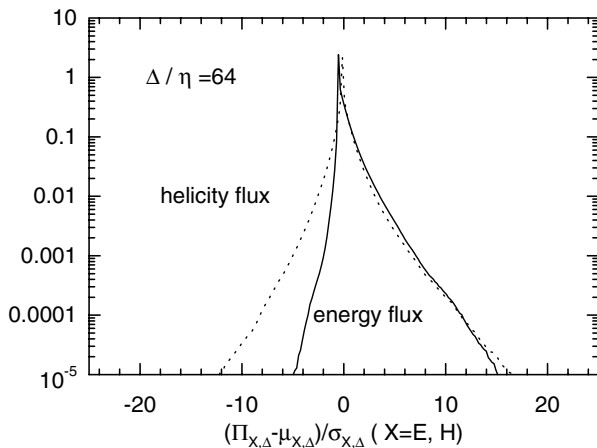


FIG. 4. 1-point PDF's of energy and helicity fluxes [$\mu_{X,\Delta} = \langle \Pi_{X,\Delta} \rangle$, $\sigma_{X,\Delta} = \sqrt{\langle (\Pi_{X,\Delta})^2 \rangle - \langle \Pi_{X,\Delta} \rangle^2}$].

and can be both positive and negative, while kinetic energy is always positive. Therefore, the long tail of helicity flux to the left does not indicate backward transfer of positive helicity but instead forward transfer of negative helicity. This argument can be made precise by means of the *helical decomposition* of the velocity field [25]. One sets $\mathbf{u} = \mathbf{u}^+ + \mathbf{u}^-$ with $\mathbf{u}^\pm(\mathbf{x}, t) = \sum_{\mathbf{k}} a_\pm(\mathbf{k}) \mathbf{h}_\pm(\mathbf{k}) e^{i\mathbf{k} \cdot \mathbf{x}}$, where $\mathbf{h}_s(\mathbf{k})$ for $s = \pm$ are eigenvectors of the curl: $i\mathbf{k} \times \mathbf{h}_s(\mathbf{k}) = s|\mathbf{k}|\mathbf{h}_s(\mathbf{k})$. As shown in Ref. [25], the + modes carry only positive helicity and the - modes only negative helicity. If we likewise decompose vorticity as $\boldsymbol{\omega} = \boldsymbol{\omega}^+ - \boldsymbol{\omega}^-$, we can define

$$\begin{aligned} \Pi_{E,\Delta}^\pm(\mathbf{x}, t) &= -\nabla \mathbf{u}^\pm(\mathbf{x}, t) : \boldsymbol{\tau}(\mathbf{x}, t), \\ \Pi_{H,\Delta}^\pm(\mathbf{x}, t) &= -2\nabla \boldsymbol{\omega}^\pm(\mathbf{x}, t) : \boldsymbol{\tau}(\mathbf{x}, t), \end{aligned} \quad (9)$$

and then $\Pi_{E,\Delta}^s$ represents flux of energy from the large-scale s modes into the small scales and $\Pi_{H,\Delta}^s$ represents the like quantity for helicity, with $s = \pm$. See Ref. [26].

In Fig. 5(a) are plotted the 1-point PDF's of $\Pi_{H,\Delta}^\pm$ for nonzero mean helicity with the inset for zero mean helicity. It may be seen that the PDF's of the + mode and - mode are skewed to the right, indicating that helicity from these two modes prefers to cascade forward to smaller scales. Likewise, in Fig. 5(b) the energy flux in both + and - modes is skewed to the right. There is somewhat less skewness in the - mode because relatively little energy is being injected into that channel for the

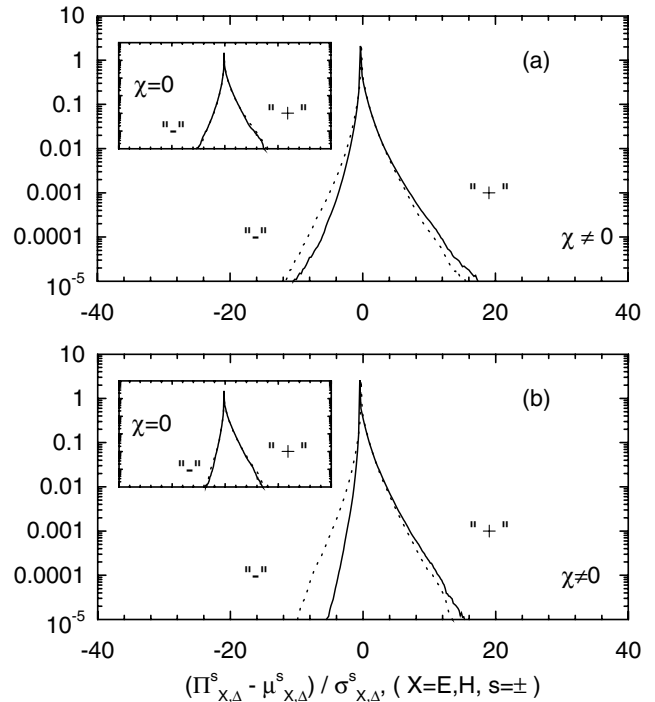


FIG. 5. 1-point PDF's of (a) \pm helicity fluxes and (b) \pm energy fluxes for different mean helicity inputs χ when $\Delta/\eta = 64$. The inset is for $\chi = 0.0$ [$\mu_{X,\Delta}^s = \langle \Pi_{X,\Delta}^s \rangle$, $\sigma_{X,\Delta}^s = \sqrt{\langle (\Pi_{X,\Delta}^s)^2 \rangle - \langle \Pi_{X,\Delta}^s \rangle^2}$].

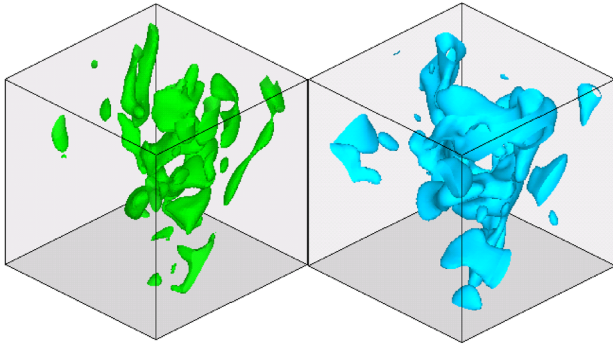


FIG. 6 (color online). Three-dimensional view of fluxes for $\Delta/\eta = 16.0$. Left: helicity flux $\Pi_{H,\Delta}/\Pi_{H,\Delta}^{\text{rms}} = 2.0$; right: energy flux $\Pi_{E,\Delta}/\Pi_{E,\Delta}^{\text{rms}} = 2.0$.

case $\chi > 0$. [The same effect is seen also for helicity flux in Fig. 5(a).] In contrast, in the inset in Fig. 5(b) is shown the + and - energy fluxes for the case $\chi = 0$. Here equal amounts of energy $\varepsilon^- = \varepsilon^+$ are injected in both channels, and the two PDF's are equally skewed. As discussed in detail in Ref. [26], this will also be asymptotically true in a long inertial range for $\chi > 0$, because the nonlinear transfer from + modes to - modes will tend to equalize the amount of energy and helicity in each and restore reflection symmetry at high wave numbers.

To see the geometric structures of the fluxes, we present a three-dimensional view of energy-flux and helicity-flux isosurfaces at $\Delta/\eta = 16.0$ in Fig. 6. Only 64^3 mesh points around the maximum energy flux region are shown. $\Pi_{E,\Delta}^{\text{rms}}$ and $\Pi_{H,\Delta}^{\text{rms}}$ are the rms energy flux and helicity flux, respectively. We can see that structures of helicity flux and energy flux are quite different. Helicity flux forms more tubelike structures than energy flux, while the latter has flatter and coarser structures. Similar tubelike and sheetlike structures have been observed for other Δ 's and they are particularly clear at smaller scales. This is consistent with the greater intermittency of helicity flux. There also appears to be a high degree of correlation between the regions of large energy and helicity flux,

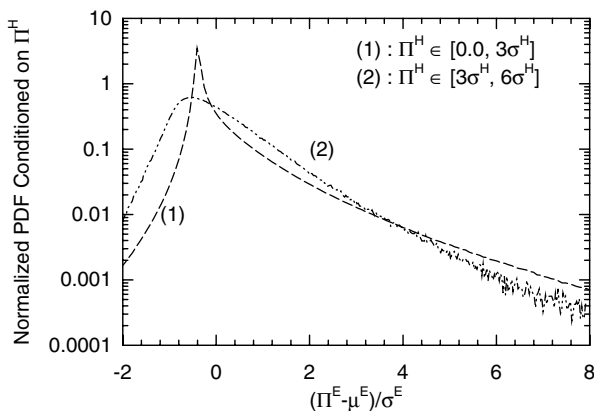


FIG. 7. Normalized energy flux PDF's conditioned on helicity flux when $\Delta/\eta = 64$, $\chi \neq 0$.

with such structures adjacent in space. However, these regions do not overlap. In fact, large fluctuations of one flux are suppressed in the regions where the other is large. For example, in Fig. 7 are shown two PDF's of energy flux, one conditioned on helicity flux in the range $[0.0, 3\sigma^H]$ and the other in the range $[3\sigma^H, 6\sigma^H]$. We can see that energy flux is more intermittent when the helicity flux is small than when the helicity flux is large. Clearly, the tail of the PDF with the large helicity flux is reduced compared to that with the small helicity flux.

We thank Robert M. Kerr, Charles Meneveau, Mark Nelkin, Xin Wang, and Victor Yakhot for helpful discussions. Simulations were performed at the cluster computer supported by NSF Grant No. CTS-0079674 at the Johns Hopkins University.

- [1] A. N. Kolmogorov, C. R. (Dokl.) Acad. Sci. URSS **32**, 19 (1941).
- [2] J. J. Moreau, C. R. Acad. Sci. Paris **252**, 2810 (1961).
- [3] H. K. Moffatt, J. Fluid Mech. **35**, 117 (1969).
- [4] M. Lautenschlager, D. P. Eppel, and W. C. Thacker, Beitr. Phys. Atmos. **61**, 87 (1988).
- [5] A. Brissaud, U. Frisch, J. Leorat, M. Lesieur, and A. Mazure, Phys. Fluids **16**, 1366 (1973).
- [6] R. H. Kraichnan, J. Fluid Mech. **59**, 745 (1973).
- [7] V. Borue and S. A. Orszag, Phys. Rev. E **55**, 7005 (1997).
- [8] L. P. Kadanoff, D. Lohse, J. Wang, and R. Benzi, Phys. Fluids **7**, 617 (1995).
- [9] P. D. Ditlevsen and P. Giuliani, Physica (Amsterdam) **280A**, 69 (2000).
- [10] L. Biferale, D. Pierotti, and F. Toschi, J. Phys. IV (France) **8**, 131 (1998).
- [11] S. Chen and X. Shan, Comput. Phys. **6**, 643 (1992).
- [12] W. Polifke and L. Shtilman, Phys. Fluids A **1**, 2025 (1989).
- [13] M. Lesieur, *Turbulence in Fluids* (Kluwer, Dordrecht, 1990).
- [14] R. H. Kraichnan, J. Fluid Mech. **62**, 305 (1974).
- [15] A. N. Kolmogorov, J. Fluid Mech. **13**, 82 (1962).
- [16] G. L. Eyink, J. Stat. Phys. **78**, 335 (1995).
- [17] C. Meneveau and J. Katz, Annu. Rev. Fluid Mech. **32**, 1 (2000).
- [18] V. Borue and S. A. Orszag, J. Fluid Mech. **366**, 1 (1998).
- [19] S. Cerutti and C. Meneveau, Phys. Fluids **10**, 928 (1998).
- [20] R. Benzi, S. Ciliberto, R. Tripiccone, C. Baudet, E. Massaioli, and S. Succi, Phys. Rev. E **48**, 29 (1993).
- [21] S. Chen, K. R. Sreenivasan, M. Nelkin, and N. Cao, Phys. Rev. Lett. **79**, 2253 (1997).
- [22] G. P. Romano and R. A. Antonia, J. Fluid Mech. **436**, 231 (2001).
- [23] K. R. Sreenivasan and R. A. Antonia, Annu. Rev. Fluid Mech. **29**, 435 (1997).
- [24] S. Chen and R. H. Kraichnan, Phys. Fluids **10**, 2867 (1998).
- [25] F. Waleffe, Phys. Fluids A **4**, 350 (1991).
- [26] Q. Chen, S. Chen, and G. L. Eyink, Phys. Fluids **15**, 361 (2003).